Redox Biology 14 (2018) 154–163

Contents lists available at ScienceDirect

Redox Biology

journal homepage: www.elsevier.com/locate/redox

Identification of novel Nrf2 activators from *Cinnamomum chartophyllum* H.W. Li and their potential application of preventing oxidative insults in human lung epithelial cells

Ming-Xing Zhou[a], Guo-Hui Li[b], Bin Sun[c], You-Wei Xu[a], Ai-Ling Li[a], Yan-Ru Li[a], Dong-Mei Ren[a], Xiao-Ning Wang[a], Xue-Sen Wen[a], Hong-Xiang Lou[a], Tao Shen[a,*]

[a] Key Lab of Chemical Biology (MOE), School of Pharmaceutical Sciences, Shandong University, Jinan, PR China
[b] Department of Pharmacy, Jinan Maternity and Child Care Hospital, Jinan, PR China
[c] National Glycoengineering Research Center, Shandong University, Jinan 250012, PR China

ARTICLE INFO

Keywords:
Cinnamomum chartophyllum
Nrf2 activator
Arsenic
Oxidative insult

ABSTRACT

Human lung tissue, directly exposed to the environmental oxidants and toxicants, is apt to be harmed to bring about acute or chronic oxidative insults. The nuclear factor erythroid 2-related factor 2 (Nrf2) represents a central cellular defense mechanism, and is a target for developing agents against oxidative insult-induced human lung diseases. Our previous study found that the EtOH extract of *Cinnamomum chartophyllum* protected human bronchial epithelial cells against oxidative insults via Nrf2 activation. In this study, a systemic phytochemical investigation of the aerial parts of *C. chartophyllum* led to the isolation of thirty chemical constituents, which were further evaluated for their Nrf2 inducing potential using NAD(P)H: quinone reductase (QR) assay. Among these purified constituents, a sesquiterpenoid bearing α, β-unsaturated ketone group, 3*S*-(+)-9-oxonerolidol (NLD), and a diphenyl sharing phenolic groups, 3, 3′, 4, 4′-tetrahydroxydiphenyl (THD) significantly activated Nrf2 and its downstream genes, NAD(P)H quinone oxidoreductase 1 (NQO-1), and γ-glutamyl cysteine synthetase (γ-GCS), and enhanced the nuclear translocation and stabilization of Nrf2 in human lung epithelial cells. Importantly, NLD and THD had no toxicities under the Nrf2 inducing doses. THD also demonstrated a potential of interrupting Nrf2-Keap1 protein–protein interaction (PPI). Furthermore, NLD and THD protected human lung epithelial cells against sodium arsenite [As(III)]-induced cytotoxicity. Taken together, we conclude that NLD and THD are two novel Nrf2 activators with potential application of preventing acute and chronic oxidative insults in human lung tissue.

1. Introduction

Oxidative stress is an imbalance of the oxidants/antioxidants tilting toward an oxidative status, and is characterized by the higher level of reactive oxygen species (ROS) and reactive nitrogen species (RNS) than normal physiological state [1]. It could be triggered by a lot of factors, e.g. heavy metals, xenobiotics, free radicals, drugs and ionizing radiation. Exposure of cells to these toxicants and oxidants impairs cellular components (e.g. lipids, proteins and nucleic acids), and initiates the pathogenesis of many diseases, including neurodegenerative diseases, cardiovascular diseases, chronic obstructive pulmonary disease (COPD), diabetes, and cancer [2–4]. Since the direct exposure to the oxidants and toxicants produced by the aggravation of environmental pollution and the increased number of smokers, human lung tissue is apt to be harmed to give rise to acute and chronic oxidative insults, which leads to the high incidences of lung diseases, such as COPD, asthma, lung cancer, pulmonary fibrosis [1,5,6]. For instance, lung cancer has become the leading cause of cancer-related deaths worldwide [7], and COPD has been estimated to be the third global leading cause of death by 2020 [6].

Activation of the nuclear factor erythroid 2-related factor 2 (Nrf2)-mediated defensive response is an effective mean of counteracting

Abbreviations: AO, acridine orange; ARE, antioxidant response element; As(III), sodium arsenite; CC, column chromatography; CHX, cycloheximide; COPD, chronic obstructive pulmonary disease; DAPI, 6-diamidino-2-phenylindole; EB, ethidium bromide; γ-GCS, γ-glutamylcysteine synthetase; GST, glutathione S-transferase; HO-1, heme oxygenase-1; Keap1, Kelch-like ECH-associated protein 1; MTT, 3-(4,5-dimethylthiazol-2-yl)-2,5-diphenyltetrazoliumbromide; NLD, 3*S*-(+)-9-oxonerolidol; NQO1, NAD(P)H: quinone oxidoreductase; Nrf2, nuclear factor erythroid 2-related factor 2; PPI, protein–protein interaction; QR, NAD(P)H: quinone reductase; RNS, reactive nitrogen species; ROS, reactive oxygen species; SF, sulforaphane; THD, 3, 3′, 4, 4′-tetrahydroxydiphenyl

* Correspondence to: School of Pharmaceutical Sciences, Shandong University, 44 Wenhua Xi Road, Jinan 250012, PR China.
E-mail address: shentao@sdu.edu.cn (T. Shen).

http://dx.doi.org/10.1016/j.redox.2017.09.004
Received 2 August 2017; Received in revised form 25 August 2017; Accepted 11 September 2017
Available online 14 September 2017

exogenous oxidative insults in lung tissues. Under basal conditions, Nrf2 binds to its repressor Kelch-like ECH-associated protein 1 (Keap1), and is maintained at a low level in cytosol through Keap1-mediated ubiquitylation and 26S proteasome-mediated degradation. When cells are exposed to oxidants and toxicants, Nrf2 is released from Keap1, translocates into the nucleus, binds to the antioxidant response element (ARE) located in the promoter region of cytoprotective genes, and activates their transcriptions [8,9]. These ARE-containing genes include: (i) intracellular redox-balancing proteins, such as γ-glutamyl cysteine synthetase (γ-GCS) and heme oxygenase-1 (HO-1) that maintain the cellular redox capacity and eliminate ROS; (ii) phase II detoxifying enzymes, including NAD(P)H: quinone oxidoreductase 1 (NQO1) and glutathione S-transferase (GST), which promote excretion of toxicants. In view of the functions of Nrf2-mediated genes, the role of Nrf2 in protection of oxidative insult-induced lung diseases has been proved by the experiments *in vivo*. Compared with Nrf2 wild-type littermate mice, Nrf2-deficient mice are more susceptible to oxidant and toxicant (e.g. arsenic, cigarette smoke, diquat)-induced insults in lung tissue [10–12]. Thus, identification of molecules that activate Nrf2-mediated defensive responses is an efficient strategy for discovering lead compounds with the therapeutic potential against oxidative stress-related lung diseases.

Natural product without doubt fulfills irreplaceable roles in drug discovery, and is invaluable source for drug candidates and leads. Plenty of natural products and 'natural product-like' chemicals demonstrated the potential as therapeutic agent against oxidative stress-related diseases, exemplified by curcumin, resveratrol, quercetin, sulforaphane [13–17]. In our continuous search of natural Nrf2 activators and investigation of their therapeutic potential on oxidative insult-induced lung diseases [17–19], the EtOH extract of *Cinnamomum chartophyllum* (Lauraceae), which is mainly distributed in the south and southeast of Yunnan province of China [20], activated Nrf2 pathway and protected human bronchial epithelial (HBE) cells against H_2O_2 and As(III)-induced cell death [18]. Importantly, no phytochemical investigation on this plant has been reported, and accordingly the chemical constituents with Nrf2 inducing effect in this plant remain unknown.

In the present research, a systematic phytochemical investigation of *C. chartophyllum* combined with aNAD(P)H: quinone reductase (QR) screening assay was performed to identify the potential Nrf2 activators of this plant. The chemical composition of *C. chartophyllum* has been illustrated for the first time, and a sesquiterpenoid bearing α, β-unsaturated ketone group, 3*S*-(+)-9-oxonerolidol (NLD), and a polyphenol, 3, 3′, 4, 4′-tetrahydroxydiphenyl (THD) with potential Nrf2 inducing effect were chosen for further studies. Our results indicated that NLD and THD significantly activated Nrf2 and its downstream genes, enhanced the nuclear translocation and stabilization of Nrf2, and protected human lung epithelial cells against sodium arsenite [As(III)]-induced cytotoxicity. Collectively, NLD and THD are two novel Nrf2 activators with potential application of preventing oxidative insults in human lung epithelial cells.

2. Materials and methods

2.1. Chemicals

Sulforaphane (SF), menadione, digitonin, As(III), and flavin adenine dinucleotide were purchased from Sigma-Aldrich (MO, USA). Cycloheximide (CHX), 4′, 6-diamidino-2-phenylindole (DAPI), 3-(4,5-dimethylthiazol-2-yl)-2,5-diphenyltetrazoliumbromide (MTT), bromophenol blue, glycerol, and bovine serum albumin (BSA) were obtained from Genview (TX, USA). Glucose-6-phosphate dehydrogenase and nicotinamide adenine dinucleoide phosphate (NADP) were purchased from Regal (Shanghai, China). β-Mercaptoethanol was obtained from Dingguo (Beijing, China). Eagle's minimal essential medium (MEM), and RPMI1640 were acquired from Gibco (CA, USA). Fetal bovine serum (FBS) was purchased from Gemini Bio-product (CA, USA). Glucose-6-phosphate and L-glutamine were obtained from Solarbio (Beijing, China).

2.2. General experimental procedures

^1H and ^{13}C NMR spectra were recorded on a Bruker Avance 600 spectrometer (Bruker, Germany) at 600 (^1H) and 150 (^{13}C) MHz, respectively. High-resolution ESI-MS mass spectra were carried out on a LTQ-Orbitrap XL instrument (Thermo, USA). Semi-preparative HPLC was performed on a Shimadzu SPD-20A instrument (Shimadzu, Japan), using an YMC-Pack ODS-A column (250 × 10 mm, 5 μm). Silica gel (200–300 mesh, Haiyang Co., Qingdao, China), and Sephadex LH-20 gel (Amersham Biosciences, USA) were used for column chromatography. Pre-coated silica GF254 plates (Haiyang Co., Qingdao, China) were used for TLC analysis.

2.3. Plant material

The aerial parts of *C. chartophyllum* were collected from Xishuangbanna, Yunnan Province, China, in September 2011, and identified by Prof. Lan Xiang, School of Pharmaceutical Sciences, Shandong University. The voucher specimen has been deposited at the Laboratory of Pharmacognosy, School of Pharmaceutical Sciences, Shandong University, under the accession number XSBN2011-ZK-02.

2.4. Extraction and isolation

The air-dried and powdered aerial parts (5.4 kg) of *C. chartophyllum* were extracted with 95% EtOH (10 L × 4). The dried EtOH extract (300.4 g) was suspended in water, partitioned successively with petroleum ether, EtOAc and n-butanol. The petroleum ether soluble partition (15.7 g) was separated over silica gel column chromatography (CC) and eluted with a gradient of petroleum ether–EtOAc to yield twenty fractions (Frs. P1–P20). Compounds **22** (12.3 mg), **23** (9.3 mg), **29** (4.1 mg), **30** (5.2 mg) and **21** (20.9 mg) were precipitated from frs. P1, P11, P6, P7, and P14, respectively. Fr. P9 was subjected to silica gel CC using a gradient of petroleum ether–EtOAc to give **27** (5.7 mg) and **28** (4.3 mg). Fr. P10 was separated on a Sephadex LH-20 column to furnish **26** (3.9 mg). Fr. P15 was chromatographed on Sephadex LH-20 to afford six subfractions (Frs. P15a–P15f). Frs. P15d and P15e were purified by semi-preparative HPLC to give **1** (3.8 mg), **3** (3.9 mg) and **8** (2.6 mg). Compounds **10** (2.4 mg), **11** (2.8 mg), **12** (2.0 mg), **17** (4.2 mg), and **19** (1.6 mg) were purified from fr. P16 by semi-preparative HPLC. Fr. P18 was fractionated by Sephadex LH-20 CC and semi-preparative HPLC to give **18** (1.0 mg).

The EtOAc-soluble partition (33.8 g) was separated on a silica gel CC using a gradient of petroleum ether–EtOAc to afford nineteen fractions (Frs. E1–E19). Compounds **24** (3.1 mg) and **25** (4.4 mg) were precipitated from frs. E8 and E9, respectively. Fr. E13 was separated by a Sephadex LH-20 CC to afford nine subfractions (Frs. E13a–E13i). Fr. E13e was purified by semi-preparative HPLC to afford **9** (2.5 mg). Fr. E13h was submitted to a Sephadex LH-20 CC and further separated by semi-preparative HPLC to give **4** (2.0 mg), **14** (10.3 mg), **15** (17.8 mg), and **20** (2.0 mg). Fr. E14 was fractionated by CC on Sephadex LH-20 and semi-preparative HPLC to yield **2** (1.5 mg), **5** (1.1 mg), **6** (2.6 mg), **7** (4.1 mg), **13** (13.5 mg), and **16** (33.0 mg). Detailed procedure on the extraction and isolation of chemical constituents from *C. chartophyllum* has been summarized in Supplementary materials.

2.5. Cell culture

Hepa 1c1c7 murine hepatoma cells, human breast carcinoma MDA-MB-231 cells, and normal human lung epithelial Beas-2B cells were obtained from American Type Culture Collection (Manassas, VA, USA). Hepa 1c1c7 cells were cultured in MEM supplemented with 10% FBS and 0.29 g/L L-glutamine. MDA-MB-231 cells and Beas-2B cells were

maintained in RPMI1640 supplemented with 10% FBS and 0.29 g/L L-glutamine. All of cells were incubated at 37 °C in a humidified incubator containing 5% CO_2.

2.6. Cell viability assay

Cells were seeded in a 96-well plate at a density of 1.0×10^4 cells/well, and were treated with indicated concentrations of NLD and THD. After culturing for the indicated time, 20 μL of MTT solution (2 mg/mL) was added to each well and incubated for additional 3 h at 37 °C. Then, the supernatant was discarded carefully, and cells containing reduced MTT were dissolved in 100 μL DMSO. After a brief period of shaking, the absorbance was measured at 570 nm on the Model 680 plate reader (Bio-Rad, CA, USA).

2.7. NAD(P)H: quinone reductase (QR) assay

Hepa 1c1c7 cells were seeded in a 96-well plate at a density of 1.0×10^4 cells/well, and were treated with indicated doses of purified constituents for 24 h. The medium was decanted, and cells were incubated with 30 μL of lysing solution [0.8% digitonin and 2 mM EDTA solution (pH 7.8)] for 15 min at 37 °C. Then, a complete reaction solution was prepared by mixing 15 mg bovine serum albumin, 6 mg MTT, 150 μL 1.5% Tween 20, 1 mL 0.5 M Tris–HCl, 15 μL 7.5 mM flavin adenine dinucleotide, 150 μL 150 mM glucose-6-phosphate, 6 μL 10 units/μL glucose-6-phosphate dehydrogenase, 15 μL 50 mM NADP, 20 μL 50 mM menadione and 18.4 mL H_2O, and was added into the cell lysates for 170 μL/well. After incubation for 4 min, a blue color was developed and the absorbance was measured at 630 nm on the Model 680 plate reader.

2.8. Dural luciferase reporter gene assay

MDA-MB-231 cells were seeded in a 24-well plate at a density of 1.5×10^5 cells/well, and were transfected with ARE-luciferase plasmid and renilla luciferase plasmid using lipofectamine 2000 (Invitrogen, CA, USA). Then, the transfected cells were treated by indicated doses of NLD and THD for 18 h. Firefly and renilla luciferase activities were measured using the Promega dual luciferase reporter gene assay system (WI, USA). Firefly luciferase activity was normalized to renilla luciferase activity, and the induction of luciferase activity was determined as a ratio compared to the control group.

2.9. Immunoblot analysis

Antibodies for Nrf2, NQO1, γ-GCS and Lamin A were purchased from Santa Cruz Biotechnology (CA, USA). Antibodies for Keap1, and β-actin were purchased from Proteintech Group (IL, USA). Cells were seeded in D35 dishes and treated with different doses of NLD and THD for the indicated time. Then, cells were lysed in sample buffer [50 mM Tris-HCl (pH 6.8), 2% SDS, 10% glycerol, 0.05 g bromophenol blue, and 10 mL β-mercaptoethanol], and were separated by SDS-PAGE on 10% gel and electrophoretically transferred into a nitrocellulose membrane (Millipore, MA, USA). Then, the membrane was blocked with 5% skim milk in PBST for 1 h at room temperature and incubated with antibodies against Nrf2, Keap1, NQO1, γ-GCS, Lamin A, and β-actin at 4 °C overnight. After rinsing, membranes were incubated with horseradish peroxidase (HRP)-conjugated secondary antibody for 1 h at room temperature. The protein bands were detected by ECL reagents using Bio-Rad ChemiDoc XRS + system (CA, USA). Chemiluminescent signal was analyzed using Image J analyze system.

2.10. Immunofluorescence

Beas-2B cells (4.0×10^4 cells/well) were seeded in a 12-well plate which have been pre-placed cell climbing pieces at the bottoms, and were treated with indicated doses of NLD and THD for 18 h. Then, the cells climbing pieces were washed with PBS and fixed with −20 °C methanol/acetone (1:1) for 10 min. The cell climbing pieces were incubated with primary rabbit anti-Nrf2 antibody at 4 °C overnight. After 3 times washing in PBS, the cell climbing pieces were incubated with Alexa Flour 594 (Proteintech Group, IL, USA) for 1 h at room temperature in the darkness, and nuclei were covered with DAPI for 10 min. The fluorescence signals were imaged using Olympus BX53 fluorescence microscope coupled to Olympus DP73 digital camera (Tokyo, Japan).

2.11. Nrf2 protein half-life measurement

The half-time of Nrf2 was analyzed by protein decay experiments. Beas-2B cells were seeded in D35 dishes and pre-incubated with or without NLD and THD for 8 h. After treatment with 50 μM CHX, cells were collected at 0, 10, 20, 30, 40 min. Then, cells were subjected to immunoblot analysis.

2.12. Glutathione (GSH) assay

Intracellular reduced glutathione (GSH) concentration was determined using the reduced glutathione assay kit (Jiancheng Bioengineering Institute, Nanjing, China). Beas-2B cells were seeded in D60 dishes, and were treated with different doses of NLD and THD for 24 h. The following procedures were carried out according to the manufacturer's instructions. All samples were carried out in triplicate for each experiment, and the value from the untreated group was set as 1.

2.13. ROS detection

The effects of NLD and THD on As(III)-induced production of ROS in Beas-2B cells were examined using ROS kits (Keygen Biotech, Nanjing, China). Beas-2B cells were incubated with indicated doses of NLD and THD for 8 h, and then treated with 5 μM As(III) for 10 h. Then, DCFH-DA (10 μM) was added for additional 30 min according to manufacturer's protocols. Cells were washed with PBS for three times, and photographed using an Olympus BX53 + DP73 fluorescence imaging system (Tokyo, Japan).

2.14. Acridine orange (AO)/ethidium bromide (EB) staining

Beas-2B cells were seeded in D35 and pre-incubated with or without indicated doses of NLD and THD for 8 h. After incubation with 5 μM As (III) for 12 h, cells were washed with PBS and stained with AO/EB according to the manufacturer's instructions (Keygen Biotech, Nanjing, China). Then, cells were photographed using an Olympus 1×71 fluorescence imaging system (Tokyo, Japan).

2.15. Annexin V-FITC /PI double staining

Beas-2B cells were seeded in D35 dishes, pre-incubated with or without indicated doses of NLD and THD for 8 h, and then were treated with 5 μM As(III) for 24 h. After being washed and harvested with PBS, cells were dissolved in 100 μL 1X binding buffer, and stained with Annexin-V and PI according to the manufacturer's instructions (BD Biosciences, CA, USA). The fluorescence was measured with excitation at 488 nm and emission at 520 nm by a FACSC alibur flow cytometer (BD Biosciences, CA, USA).

2.16. Molecular docking analysis

The crystal structure of Keap1 in complex with 3-(4-chlorophenyl) propanoic acid (PDB code 5FNQ) was downloaded from the Protein Data Bank (www.rcsb.org) [21]. The confirmations of NLD and THD

were generated using SYBYL-X, and the energy was minimized with Tripos force field and Gasteiger-Huckel charges. The cocrystalized structure was prepared using SYBYL-X. Hydrogens were added and the energy was minimized with the Amber force field and Amber charges. The docking of NLD and THD into the Keap1 binding site was performed using the GOLD program to give best-docked conformations. After docking, the new ligand-protein complex was formed through merging the best-docked conformation of NLD and THD into the ligand-free protein of Keap1, and then was subjected to energy minimization with the Amber force field and Amber charges. Finally, the ligand-protein complex was imported into PyMol software for the image optimization.

2.17. Statistical analysis

One way analysis of variance (ANOVA) and post hoc multiple comparison Bonferroni test were used to determine the significant difference between two groups. Results are presented as the mean ± SD. $P < 0.05$ was considered to be significant.

3. Results

3.1. Isolation and structure elucidation of chemical constituents

To characterize the chemical constituents with Nrf2 inducing effect, a systematic phytochemical investigation of aerial parts of *C. chartophyllum* was performed using multiple chromatographic methods. The EtOH extract was partitioned sequentially by petroleum ether, EtOAc, and n-butanol. Repeated chromatography of the petroleum ether and EtOAc extracts by silica gel CC, Sephdex LH-20 CC, and semi-preparative HPLC, led to the isolation of thirty known chemical constituents. Their structures were identified to be 3*S*-(+)-9-oxonerolidol (NLD, **1**) [22], 3, 3′, 4, 4′-tetrahydroxydiphenyl (THD, **2**) [23], L-sesamin (**3**), genkwanin (**4**), kaempferol (**5**), quercetin (**6**), 3′,4′,5,7-tetrahydroxyflavanone (**7**), 5α-hydroxy-2-oxo-p-menth-6(1)-ene (**8**), 8-hydroxycarvotanacetone (**9**), (4*R*,6*R*)-6-hydroxypiperitone (**10**), (4*S*,6*R*)-6-hydroxypiperitone (**11**), 2-methyl-6-(*p*-tolyl) heptane-2,3-diol (**12**), protocatechuic acid (**13**), isovanillic acid (**14**), ethyl protocatechuate (**15**), 1,3,5-trimethoxybenzene (**16**), 4-hydroxy-4,7-dimethyl-1-tetralone (**17**), rel-(3*R*,3′*S*,4*R*,4′*S*)-3,3′,4,4′-tetrahydro-6,6′-dimethoxy[3,3′-bi-2H-benzopyran]-4,4′-diol (**18**), (-)-piperitol (**19**), 5,7-dihydroxychromone (**20**), β-sitosterol (**21**), n-dotriacontane (**22**), n-octacosanol (23), n-dotriacontanol (**24**), n-eicosanic acid (**25**), lignoceric acid (**26**), hexacosanoic acid (**27**), heptacosanoic acid (**28**), octacosyl palmitate (**29**), and dotriacontanyl hexadecanoate (**30**), by comparison of their NMR and MS data with those reported in the literature (Supplementary materials). The chemical structures of purified constituents (**1–30**) have been shown in Fig. 1 and S1 (Supplementary materials).

3.2. Evaluation of Nrf2 inducing effects of purified constituents

To evaluate the Nrf2 inducing effect of purified constituents, we established a cell-based bioassay via measuring QR activity in heap 1c1c7 murine hepatoma cells [19]. The data in the untreated control group were normalized as 1, and QR inducing activity of tested constituents was represented by the maximum folds of QR inducing activity (MQI) compared with the untreated control group. 1.5-fold of QR inducing activity (MQI = 1.5) under the tested doses was adopted as a criterion for the bioactive constituents. All of the purified constituents (**1–30**) were subjected to the QR inducing assay, and only six compounds, including a sesquiterpenoid (NLD, **1**), a biphenyl (THD, **2**), a lignan (**3**), and three flavonoids (**4–6**) demonstrated dose-dependent QR inducing effect with MQI ranging from 1.60 to 2.39 (Fig. 1). Compared to the positive control SF with an approximately 2.8-fold induction at 2.0 μM, these constituents displayed moderate QR inducing activities, but possessed broad effective dose range. The maximum untoxic doses were > 100 μM for **1–4**, 50 μM for **5**, and 25 μM for **6** against heap 1c1c7 cells. These results suggested that constituents **1–6** displayed the potential of the Nrf2 induction, and might be the substances supporting the Nrf2 inducing effect of the *C. chartophyllum* extract.

To illustrate the mechanism of Nrf2 induction and preventive potential of bioactive constituents, we have selected NLD (**1**) previously reported from *Magnolia kobus* [22], and THD (**2**) previously isolated *Cinnamomum cassia* [23], for further investigation. The reasons for the selection are: (i) NLD and THD possess high potency on QR induction (MQIs > 2.0), and have low toxicities (minimum inhibition concentrations > 100 μM); (ii) NLD and THD are novel Nrf2 activators, which have not been reported previously; (iii) although more potent than NLD and THD, flavonoids (**4–6**), are well-known Nrf2 activators that are lack of novelty. Therefore, detailed studies on the Nrf2 activation and cellular protection of NLD and THD have been performed.

3.3. Identification of NLD and THD as Nrf2 activators using human breast carcinoma cells

Previous to further studies, we confirmed the Nrf2 inducing potency of NLD and THD using human breast carcinoma MDA-MB-231 cell line, which was sensitive in response to Nrf2 inducers [24]. We first evaluated the cytotoxicity of NLD and THD against MDA-MB-231 cells using the MTT assay. As shown in Fig. 2A, when cells were treated with NLD and THD for 24 h, no evident toxicities were observed below 100 μM, and accordingly the doses < 50 μM were selected for further study. Next, a dual-luciferase reporter gene assay was adopted to investigate Nrf2 induction by NLD and THD in MDA-MB-231 cells. Both NLD and THD induced the transcriptional activity of Nrf2 in a dose-dependent manner (Fig. 2B). The maximum inductions were about 2.5-fold for NLD, and 3.0-fold for THD at 50 μM. Similarly, the protein levels of Nrf2 and its downstream genes, NQO1 and γ-GCS, dose-dependently increased after exposure of cells to NLD and THD for 18 h (Fig. 2C). These data confirmed that NLD and THD were two activators of Nrf2 signaling pathway.

3.4. NLD and THD activate Nrf2 signaling pathway in human lung epithelial cells

Since the direct exposure to the environmental oxidants and toxicants, the lung is the major target organ for oxidative insults and carcinogenicity. Nrf2-mediated cytoprotection plays adominant role for lung tissue counteracting oxidative damages, and therefore the capacity of NLD and THD to activate the Nrf2 pathway has been investigated in human normal lung epithelial Beas-2B cells. We first detected the toxicity of NLD and THD in Beas-2B cells to determine the treatment doses. When cells were exposed to NLD and THD for 48 h, there was no significant toxicities below 100 μM for NLD, and 25 μM for THD (Fig. S2 in Supplementary materials). Thus, the doses ≤ 100 μM for NLD, and ≤ 25 μM for THD were chosen for subsequent Beas-2B cell-based assay. We have also detected the protein levels of Nrf2, Keap1, NQO1 and γ-GCS in response to the NLD and THD treatments for 18 h under the doses ranging from 0.39 to 100 μM (Fig. 3A). When cells were exposed to NLD, the expressions of Nrf2, NQO1 and γ-GCS could be induced at 1.56 μM and reached the maximum levels at 50 μM. Similarly, Nrf2-mediated cytoprotective genes were activated by THD at 0.78 μM, and reached its climax at 25 μM. The decreased protein levels of these two constituents at high doses were caused by the cytotoxicity. Both NLD and THD had no effect on Keap1 protein levels under the tested doses. Next, the time dependent inductions of Nrf2, Keap1, NQO1 and γ-GCS by NLD and THD were investigated (Fig. 3B). The protein level of Nrf2 in cells treated by NLD and THD increased as early as 4 h, reached the highest level at 24 h, and then gradually decreased to the basal level. The two downstream genes, NQO1 and γ-GCS, demonstrated

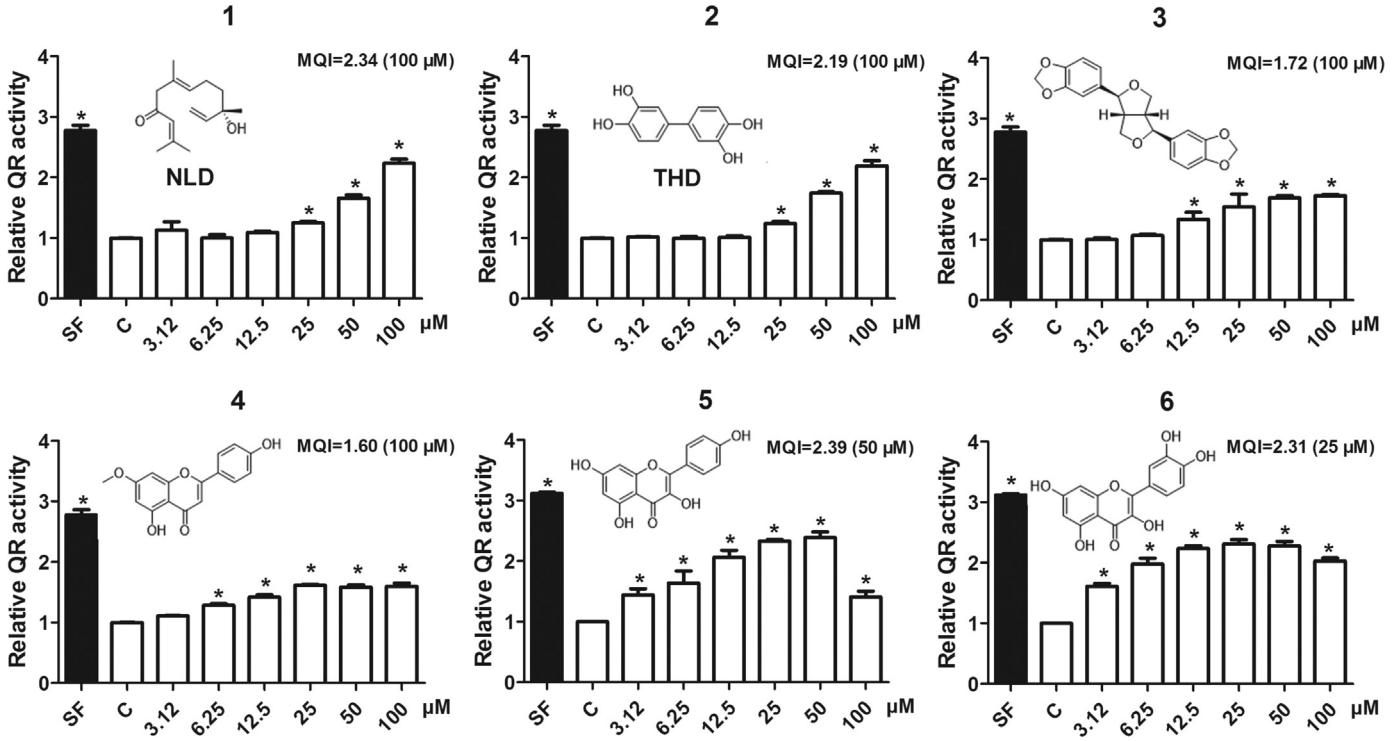

Fig. 1. Evaluation of Nrf2 inducing effects of purified constituents from the aerial parts of *C. chartophyllum*. Hepa 1c1c7 cells were used for evaluation of QR inducing activity. Cells were treated with indicated doses of constituents for 24 h before QR inducing activities were determined. SF (2.0 μM) was used as a positive control. Results are expressed as mean ± SD (n = 3). *p < 0.05 treated versus control.

continuous upregulation, and reached the maximum level at 36 h. Again, no effect on Keap1 protein expression was observed. When cells are exposed to activators, Nrf2 translocates into the nucleus and induces the transcription of a series of target genes. Therefore, we investigated whether NLD and THD could induce Nrf2 nuclear translocation using immunofluorescence assay. As expected, Nrf2 proteins were mainly localized in the cytoplasm in the control group, and were accumulated in the nucleus after NLD and THD treatments (Fig. 3C). Next, to investigate the effect on stabilization of Nrf2 protein, we tested the half-life of Nrf2 in presence or absence of NLD and THD (12.5 μM). As shown in Fig. 3D, the half-life of Nrf2 in the basal condition was about 14.7 min; however, the half-life of Nrf2 increased to 25.8 min and 31.7 min after NLD and THD treatments. Collectively, these results suggested that NLD and THD induced expression of Nrf2 and its target genes by enhancing the nuclear translocation, stabilizing Nrf2 protein, and upregulating Nrf2 at the protein level in lung epithelial cells.

3.5. THD has the potential of interrupting Nrf2-Keap1 protein–protein interaction

Since Nrf2-Keap1 protein–protein interaction (PPI) has been regarded to be a key point for regulating Nrf2 activation, the molecular docking analysis was performed to determine whether the activation of Nrf2 might be attributed to direct inhibition of Nrf2-Keap1 PPI. NLD possessed a chain sesquiterpenoid skeleton, which is flexible and unreasonable as a PPI inhibitor. Only THD was subjected to the docking analysis to determine its potential binding mode to the Keap1. We firstly analyzed the Keap1 domains and their functions, and confirmed the Keap1 kelch domain to be the binding site (Fig. 4A). Next, the Keap1 cocrystal was downloaded, and the docking analysis was completed using SYBYL-X, Gold, and PyMol programs. The docking mode of THD in the binding site of Keap1 (PDB code 5FNQ) has been displayed in Fig. 4B (front view) and 4 C (top view). As shown in Fig. 4D, there were three hydrogen bond interactions between THD and amino acid residues in Keap1. The three interactions were hydrogens at 1, 2, 1′-hydroxyl groups of THD to Leu365, Ser508, and Leu557 in Keap1, with the distances of 1.6 Å, 2.4 Å, and 1.7 Å, respectively. These results implied that THD might possess capability of interrupting Nrf2-Keap1 PPI attributing to the activation of Nrf2 pathway.

3.6. NLD and THD protect human lung epithelial cells against As(III)-induced cytotoxicity

To examine the feasibility of using NLD and THD for prevention against environmental toxicant-induced lung tissue damage, these two Nrf2 activators, NLD and THD, have been tested in an As(III)-induced cytotoxicity model *in vitro*. Firstly, we tested the effectiveness of NLD and THD in protecting Beas-2B cells against As(III)-induced cell death. As shown in Fig. 5A, pretreatments with indicated doses of NLD and THD for 8 h significantly inhibited cell death in response to 10 μM As (III) treatment, and pretreatments with 25 μM NLD and 1.56 μM THD achieved the best protective effect. Importantly, treatment of cells with 25 μM NLD and 1.56 μM THD alone could activate Nrf2-mediated cytoprotection without any cytotoxicity (Fig. S2), and thus were chosen for the subsequent experiments. Next, after pretreatments of NLD (25 μM) and THD (1.56 μM) for 8 h, Beas-2B cells were treated with the indicated does of As(III). NLD and THD significantly improved cell survival (Fig. 5B). In addition, NLD and THD dose-dependently increased the intracellular reduced GSH level (Fig. 5C). Since As(III)-induced toxicity was caused by upregulation of ROS, we measured the intracellular ROS level [25]. Treatment with 5 μM As(III) alone significantly enhanced ROS levels, but it could be reverted by pretreatment with 25 μM NLD and 1.56 μM THD (Fig. 5D). While these two doses for NLD and THD alone had no impact on ROS levels (Fig. 5D). Finally, we determined the effect of NLD and THD on As(III)-induced apoptotic cell death. As depicted in Fig. 5E, AO/EB staining indicated that 5 μM As(III) treatment increased the number of apoptotic cells, whereas pretreatments with NLD (25 μM) and THD (1.56 μM) blocked the increase of apoptotic cell number. Apoptotic cell death was quantified using Annexin V-FITC/PI flow cytometry, which confirmed the

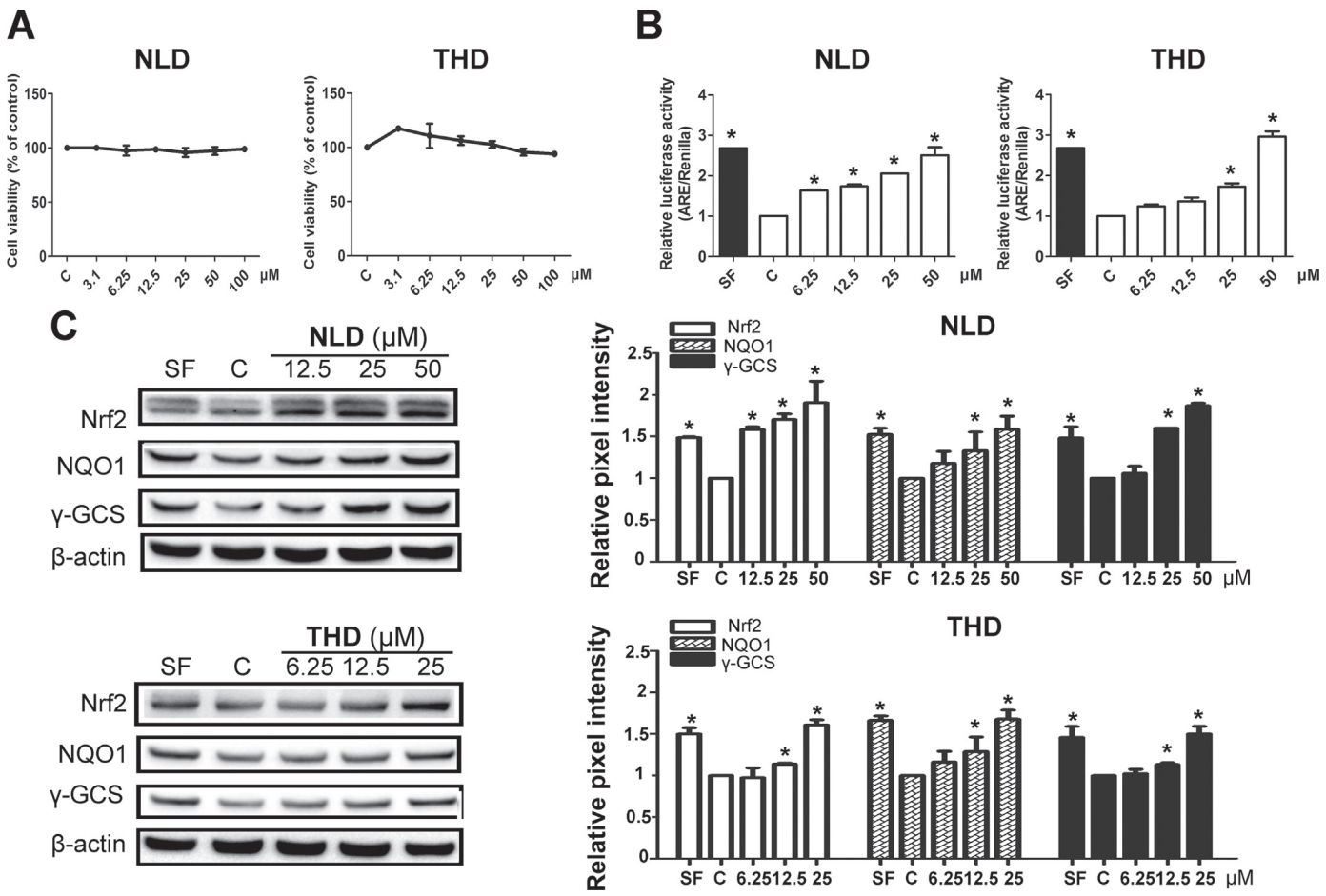

Fig. 2. Identification of NLD and THD as Nrf2 activators in human breast carcinoma cells. (A) NLD and THD had no cytotoxicities up to 100 μM. MDA-MB-231 cells were treated with different doses of NLD and THD for 24 h, and then cell viability was examined by the MTT assay. (B) NLD and THD induced ARE-luciferase activity in a dose-dependent manner. MDA-MB-231 cells were transfected with ARE-luciferase plasmid and renilla luciferase expression plasmid, and then treated by different concentrations of NLD and THD for 18 h. (C) NLD and THD dose-dependently induced the protein expressions of Nrf2, NQO1, and γ-GCS. Cells were treated by indicated doses of NLD and THD for 18 h, and then total cell lysates were determined by immunoblot analysis. SF (5.0 μM) was used as a positive control. Results are expressed as mean ± SD (n = 3). *$p < 0.05$ treated versus control.

protection of NLD and THD against As(III)-induced damages (Fig. 5F). It is noted that NLD and THD alone have no effect on cell apoptosis. Taken together, these results demonstrated that NLD and THD were able to enhance intracellular redox capacity, inhibit As(III)-induced oxidative stress, and protect lung epithelial cells against As(III)-induced toxicity.

4. Discussion

Cinnamomum chartophyllum enjoys limited regional distribution in China [20], and few findings on its phytochemical and pharmacological aspects have been reported. In the present research, we have identified thirty constituents from this plant, including six terpenoids (**1**, **8**–**12**), one diphenyl (**2**), two lignans (**3** and **19**), four flavonoids (**4**–**7**), four aromatic compounds (**13**–**16**), one naphthalenone derivative (**17**), two chromone derivatives (**18** and **20**), one steroid (**21**), and nine aliphatic compounds (**22**–**30**) (Fig. 1 and S1). To our knowledge, this is the first report on the chemical composition of this plant. Surprisingly, *C. chartophyllum* did not contain the cinnamonyl-based constituents (e.g. cinnamaldehyde), a group of substances responsible for the biological functions (particularly the Nrf2 inducing effect) of the plants from genus *Cinnamomum* [26–28]. This unexpected finding implied that *C. chartophyllum* contained undiscovered Nrf2 activators.

QR is a phase II detoxifying enzyme possessing the capability of protecting cells and tissues against oxidants and toxicants (e.g. quinones and electrophilic compounds), and is regulated by Nrf2 [29,30]. Herein, with the exception of the well-known Nrf2 activators flavonoids (**4**–**6**) and a lignan (**3**), NLD and THD demonstrated QR inducing activities for the first time (Fig. 1) [13]. Thus, it was concluded that the Nrf2 inducing effect and the protective effect against oxidative insults of the EtOH extract of *C. chartophyllum* were attributed to the combined effects of terpenoid (**1**), diphenyl (**2**), lignan (**3**), and flavonoids (**4**–**6**) [18]. Currently, the known Nrf2 activators are classified into ten classes based on their structures [15,16]. Based on this theory, NLD and THD belong to the two distinct groups, which are the Michael acceptor for NLD and the polyphenol for THD. Since their significant QR inducing effects and the rare findings on their biological aspects, NLD and THD were chosen for the further investigation. We adopted MDA-MB-231 cell line, which was suitable for identification of Nrf2 activators because of a very low basal cellular Nrf2 level [17,18], to confirm the inductions of Nrf2-mediated defensive system by NLD and THD. Consistent with the QR assay, NLD and THD activated the Nrf2 pathway (Fig. 2).

Cumulative evidences have proved that Nrf2 is highly expressed in relative abundance in human lung tissue, to counteract the insults caused by environmental oxidants and toxicants [31]. Plenty of Nrf2 inducers, exemplified by SF, resveratrol, xanthohumol, tanshinone I, bis [2-hydroxybenzylidene]acetone, have demonstrated protective and therapeutic effects on lung disorders [10,17,32–34]. Nrf2 is a good target for discovering agents possessing therapeutic effect on human lung diseases [35–37]. In this study, experiments *in vitro* were performed using Beas-2B cells to evaluate the Nrf2 inducing effect of NLD and THD on human normal lung tissue. We have found that NLD and

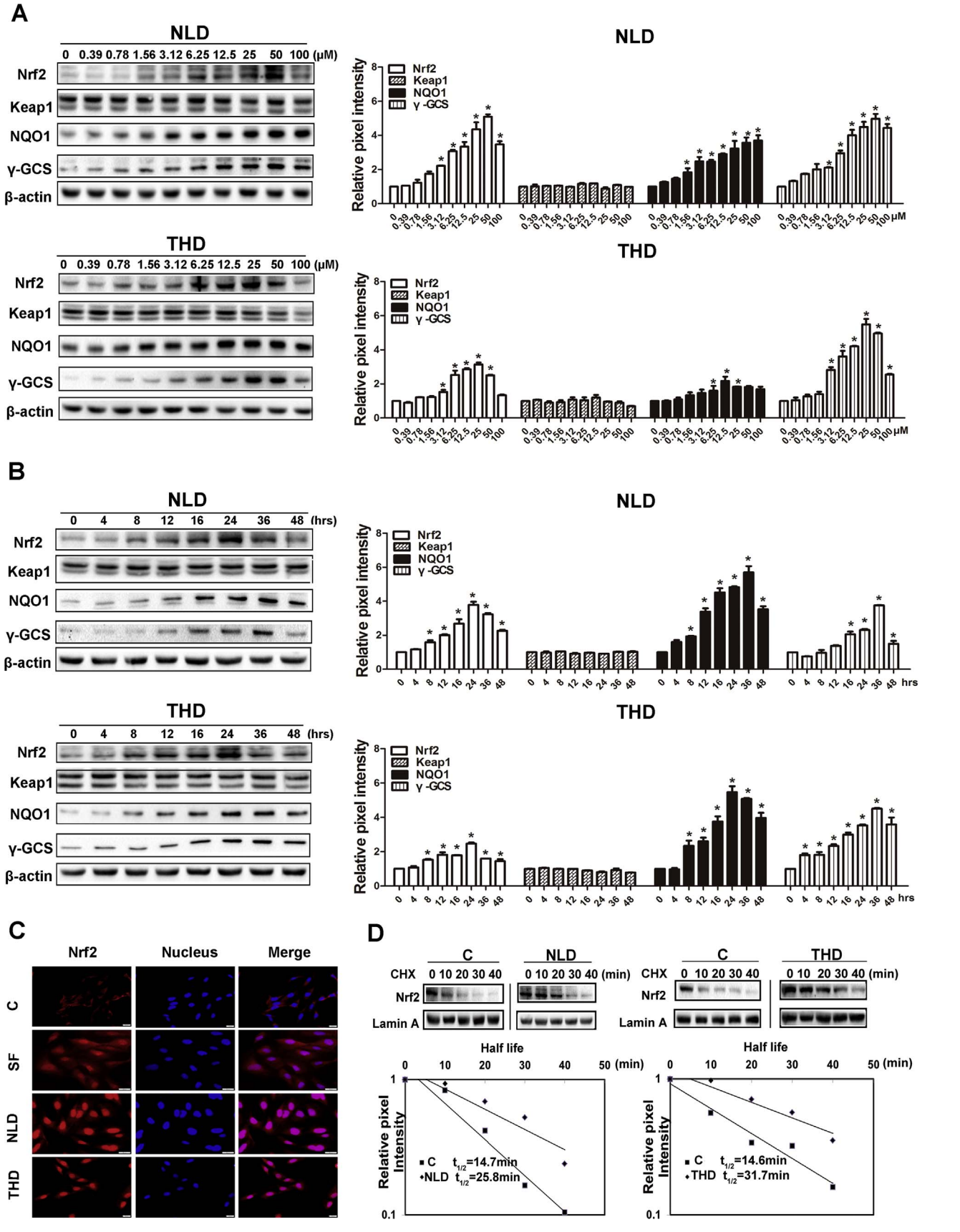

(caption on next page)

Fig. 3. NLD and THD activated Nrf2 signaling pathway in human lung epithelial cells. (A) NLD and THD dose-dependently induced the expressions of Nrf2, NQO1, and γ-GCS, but had no effect on Keap1. Cells were treated by indicated doses of NLD and THD for 18 h, and then total cell lysates were analyzed by immunoblot analysis. (B) NLD and THD induced Nrf2, NQO1, and γ-GCS, but had no effect on Keap1 in the time course study. Beas-2B cells were treated with NLD and THD at 12.5 μM for the indicated duration, and total cell lysates were subjected to immunoblot analysis. Results are expressed as mean ± SD (n = 2). *p < 0.05 treated versus control. (C) NLD and THD induced the nuclear translocation of Nrf2. Beas-2B cells were pre-incubated with or without NLD and THD (12.5 μM) for 18 h, and then subjected to indirect fluorescence staining. SF (5.0 μM) was used as a positive control. (D) NLD and THD increased the half-life of Nrf2. Beas-2B cells were left untreated or treated with NLD and THD (12.5 μM) for 8 h. CHX (50 μM) was added to block protein synthesis. Cells were harvested at the indicated time point, and total cell lysates were subjected to immunoblot analysis.

THD significantly activated Nrf2 and its downstream genes, NQO1, and γ-GCS, and enhanced the nuclear translocation and stabilization of Nrf2 in human lung epithelial Beas-2B cells (Fig. 3). According to these data, NLD and THD are verified to be canonical Nrf2 activators. More importantly, NLD and THD had no toxicity under the Nrf2 inducing doses in Beas-2B cells, and had a broad effective dose range (Fig. 3A and S2). Furthermore, NLD and THD-mediated Nrf2 activations in Beas-2B cells are intermittent (Fig. 3B), which are similar to that of chemopreventive agents (e.g. SF), but different from that of toxicants and carcinogens [38].

Nrf2-Keap1 PPI is an important Keap1-dependent mechanism for regulating Nrf2 activation [16,39]. The kelch domains of Keap1 homodimer associate with the Neh2 domain of Nrf2 [8]. Some peptides that mimic the Nrf2 protein were able to disrupt Keap1-Nrf2 PPI and activate Nrf2 pathway [40, 41]. Presently, seeking Nrf2-Keap1 PPI inhibitors using the virtual screening method and computational approaches represents a promising strategy to discover Nrf2 inducers. It promoted the discovery of plenty of small molecules to be Nrf2 activators through interrupting Nrf2-Keap1 PPI [38,42,43]. Our data indicated that THD interacted with three bonds in the kelch domain of Keap1, and demonstrated a potential capability of interrupting Nrf2-Keap1 PPI (Fig. 4).

Arsenic is a ubiquitous environmental contaminant existed in groundwater, soil and dust, which poses a dreadful threat to human across the world [44]. Exposure to arsenic gives rise to many health disorders, such as cancer, diabetes, chronic inflammation and hypertension, in various human organ systems. Among them, the lung is the major target organ for arsenic-induced acute or chronic toxicities [45–48]. Emerging evidences indicated that arsenic induced lung injury since its ability to generate ROS and elevate oxidative burden by disturbing the antioxidant/oxidant balance in lung [49]. We next investigated whether NLD and THD could be used as agents to protect cells against As(III)-induced oxidative insults in human lung epithelial Beas-2B cells. GSH is an endogenous antioxidant with the abilities of scavenging intracellular ROS and thus preventing damages to cellular components caused by ROS [50]. As shown in Fig. 5, NLD and THD treatments enhanced GSH levels and reduced As(III)-induced ROS levels. The effect of upregulating GSH level by NLD and THD was consistent with their function on increasing protein expression of γ-GCS, which was a key enzyme for GSH synthesis [51]. Because ROS are involved in the As(III)-induced cytotoxicity, inhibition of the ROS production by NLD and THD definitely enhanced cell viability, and reduced cell apoptosis caused by the exposure to As(III). These results supported the potential uses of NLD and THD for the prevention of oxidative stress in human lung tissue.

5. Conclusions

In summary, our findings indicated that sesquiterpenoid, biphenyl, lignan, and flavonoids contributed to the reported preventive effect of

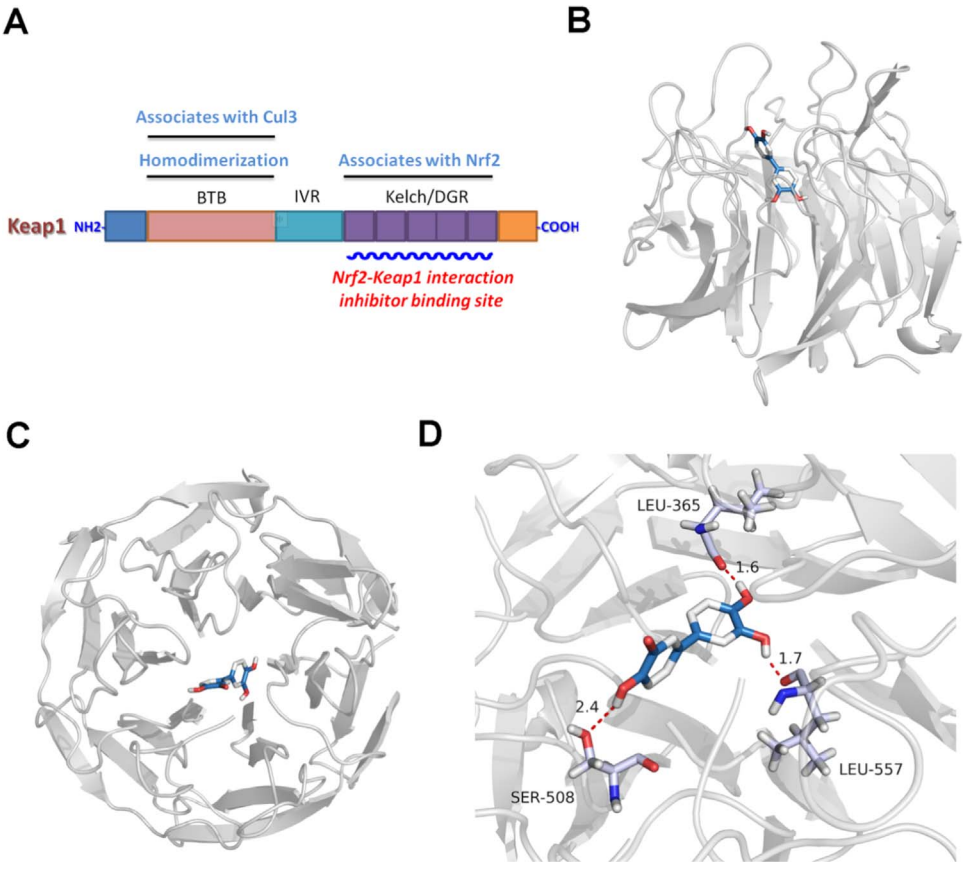

Fig. 4. Proposed docking mode of THD in the binding site of Keap1 (PDB code 5FNQ). (A) Domain structure of Keap1 and their functions. Keap1 contains three major domains, which are BTB, IVR and Kelch/DGR. The BTB domain involves in Keap1 homodimerization and associates with Cul3. The IVR domain connects the BTB domain with Kelch/DGR domain. The Kelch/DGR domain mediates binding with the Neh2 domain of Nrf2, and is the Nrf2-Keap1 interaction inhibitor binding site. (B) Front view, and (C) top view of the docking mode of THD in the binding site of Keap1. (D) The potentials interaction between THD and Keap1 via hydrogen bonds. Keap1 was shown in cartoon representation. THD and key amino acid residues in Keap1 were shown in sticks. Potential hydrogen bonds were depicted in red dot lines and the distances (Å) were labeled. The binding mode was derived from SYBYL-X and GOLD programs, and the images were generated by PyMol software.

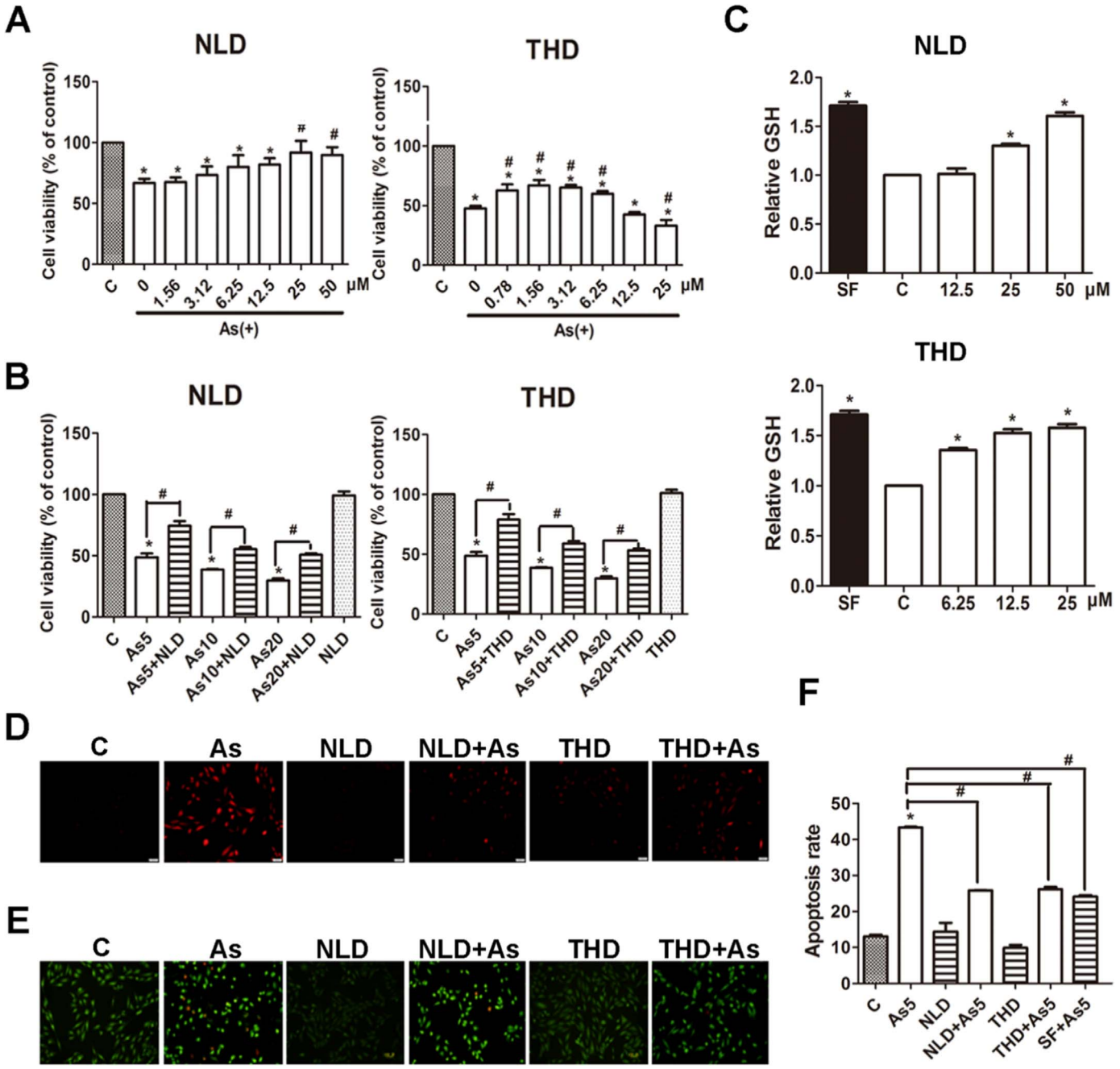

Fig. 5. NLD and THD protect human lung epithelial cells against As(III)-induced cytotoxicity. (A, B) NLD and THD protected Beas-2B cells against As(III)-induced cell death. For A, Beas-2B cells were pretreated with indicated doses of NLD and THD for 8 h and treated with 10 μM As(III) for 24 h. For B, Beas-2B cells were pretreated with NLD (25 μM) and THD (1.56 μM) for 8 h and then treated with the indicated does of As(III) for 24 h. Cell viability was measured using the MTT assay. (C) NLD and THD increased intracellular GSH levels. Beas-2B cells were treated with indicated doses for 24 h, and the levels of reduced GSH were analyzed using GSH detection kits. SF (5 μM) was used as a positive control. (D) NLD and THD reduced the As(III)-induced upregulation of intracellular ROS level. Beas-2B cells were pretreated with NLD (25 μM) and THD (1.56 μM) for 8 h and then treated with 5 μM As(III) for 10 h. The level of ROS was determined using the ROS detection kits. (E, F) NLD and THD inhibited As(III)-induced cell apoptosis. Beas-2B cells were left untreated or pretreated with NLD (25 μM) and THD (1.56 μM) for 8 h and then treated with 5 μM As(III). Apoptotic cell death was detected using AO/EB staining with fluorescence microscope (E) or Annexin V-FITC/PI staining with flow cytometry (F). SF (2 μM) was used as a positive control. Results were expressed as mean ± SD (n = 3). *$p < 0.05$ treated versus control; #$p < 0.05$ treated versus As (III).

C. chartophyllum against oxidative insults via Nrf2 activation. The sesquiterpenoid NLD and the biphenyl THD are novel Nrf2 activators identified for the first time in this research, and also display the potential of these two newly identified Nrf2 activators as preventive agents against As(III)-induced oxidative stress in Beas-2B cells. Our results implied the potential applications of *C. chartophyllum* against oxidative stress-related diseases (e.g. COPD, diabetes, cardiovascular diseases). Future directions call for a further biological evaluation to illustrate the detailed mechanisms by which NLD and THD activate the Nrf2 pathway, and a sufficient pharmacological investigation *in vivo* to confirm the prevention of NLD and THD, as well as *C. chartophyllum* against oxidative stress-induced diseases.

Conflict of interest

The authors declare that there is no conflict of interest.

Supplementary materials

Detailed procedure on the extraction and isolation of chemical constituents from *C. chartophyllum*, as well as the chemical structures of purified constituents has been summarized in Supplementary Materials.

Acknowledgments

This work was supported by NNSFs of China (31470419 and 81673558), NSF of Shandong Province (ZR2014HM019), and Young Scholars Program of Shandong University (2015WLJH50).

Appendix A. Supporting information

Supplementary data associated with this article can be found in the online version at http://dx.doi.org/10.1016/j.redox.2017.09.004.

References

[1] E. Bargagli, C. Olivieri, D. Bennett, A. Prasse, J. Muller-Quernheim, P. Rottoli, Oxidative stress in the pathogenesis of diffuse lung diseases: a review, Respir. Med. 103 (2009) 1245–1256.
[2] N. Simonian, J. Coyle, Oxidative stress in neurodegenerative diseases, Annu. Rev. Pharmacol. Toxicol. 36 (1996) 83–106.
[3] D. Jay, H. Hitomi, K.K. Griendling, Oxidative stress and diabetic cardiovascular complications, Free Radic. Biol. Med. 40 (2006) 183–192.
[4] J.E. Repine, A. Bast, I. Lankhorst, O.S.S. Group, Oxidative stress in chronic obstructive pulmonary disease, Am. J. Respir. Crit. Care Med. 156 (1997) 341–357.
[5] W. MacNee, Oxidative stress and lung inflammation in airways disease, Eur. J. Pharmacol. 429 (2001) 195–207.
[6] A. Lopez, K. Shibuya, C. Rao, C. Mathers, A. Hansell, L. Held, V. Schmid, S. Buist, Chronic obstructive pulmonary disease: current burden and future projections, Eur. Respir. J. 27 (2006) 397–412.
[7] L.A. Torre, F. Bray, R.L. Siegel, J. Ferlay, J. Lortet-Tieulent, A. Jemal, Global cancer statistics, 2012, CA Cancer J. Clin. 65 (2015) 87–108.
[8] M.C. Jaramillo, D.D. Zhang, The emerging role of the Nrf2–Keap1 signaling pathway in cancer, Genes Dev. 27 (2013) 2179–2191.
[9] A. Lau, N.F. Villeneuve, Z. Sun, P.K. Wong, D.D. Zhang, Dual roles of Nrf2 in cancer, Pharmacol. Res. 58 (2008) 262–270.
[10] Y. Zheng, S. Tao, F. Lian, B.T. Chau, J. Chen, G. Sun, D. Fang, R.C. Lantz, D.D. Zhang, Sulforaphane prevents pulmonary damage in response to inhaled arsenic by activating the Nrf2-defense response, Toxicol. Appl. Pharmacol. 265 (2012) 292–299.
[11] K.C. Wu, Y. Zhang, C.D. Klaassen, Nrf2 protects against diquat-induced liver and lung injury, Free Radic. Res. 46 (2012) 1220–1229.
[12] T. Iizuka, Y. Ishii, K. Itoh, T. Kiwamoto, T. Kimura, Y. Matsuno, Y. Morishima, A.E. Hegab, S. Homma, A. Nomura, Nrf2-deficient mice are highly susceptible to cigarette smoke-induced emphysema, Genes Cells 10 (2005) 1113–1125.
[13] H. Kumar, I.-S. Kim, S.V. More, B.-W. Kim, D.-K. Choi, Natural product-derived pharmacological modulators of Nrf2/ARE pathway for chronic diseases, Nat. Prod. Rep. 31 (2014) 109–139.
[14] B. Jagatha, R.B. Mythri, S. Vali, M.S. Bharath, Curcumin treatment alleviates the effects of glutathione depletion *in vitro* and *in vivo*: therapeutic implications for Parkinson's disease explained via in silico studies, Free Radic. Biol. Med. 44 (2008) 907–917.
[15] W. Hur, N.S. Gray, Small molecule modulators of antioxidant response pathway, Curr. Opin. Chem. Biol. 15 (2011) 162–173.
[16] S. Magesh, Y. Chen, L. Hu, Small molecule modulators of Keap1-Nrf2-ARE pathway as potential preventive and therapeutic agents, Med. Res. Rev. 32 (2012) 687–726.
[17] T. Shen, T. Jiang, M. Long, J. Chen, D.-M. Ren, P.K. Wong, E. Chapman, B. Zhou, D.D. Zhang, A curcumin derivative that inhibits vinyl carbamate-induced lung carcinogenesis via activation of the Nrf2 protective response, Antioxid. Redox Signal. 23 (2015) 651–664.
[18] T. Shen, X.-M. Chen, B. Harder, M. Long, X.-N. Wang, H.-X. Lou, G.T. Wondrak, D.-M. Ren, D.D. Zhang, Plant extracts of the family Lauraceae: a potential resource for chemopreventive agents that activate the nuclear factor-erythroid 2-related factor 2/antioxidant response element pathway, Planta Med. 80 (2014) 426–434.
[19] M.-X. Zhou, X. Wei, A.-L. Li, A.-M. Wang, L.-Z. Lu, Y. Yang, D.-M. Ren, X.-N. Wang, X.-S. Wen, H.-X. Lou, Screening of traditional Chinese medicines with therapeutic potential on chronic obstructive pulmonary disease through inhibiting oxidative stress and inflammatory response, BMC Complement. Altern. Med. 16 (2016) 360.
[20] S. Chen, M. Gilbert, Flora of China, Science, Beijing and Missouri Botanical Garden Press, St Louis, 2006.
[21] T.G. Davies, W.E. Wixted, J.E. Coyle, C. Griffiths-Jones, K. Hearn, R. McMenamin, D. Norton, S.J. Rich, C. Richardson, G. Saxty, Monoacidic inhibitors of the Kelch-like ECH-associated protein 1: nuclear factor erythroid 2-related factor 2 (KEAP1: NRF2) protein–protein interaction with high cell potency identified by fragment-based discovery, J. Med. Chem. 59 (2016) 3991–4006.
[22] T. Iida, M. Nakano, K. Ito, Hydroperoxysesquiterpene and lignan constituents of *Magnolia kobus*, Phytochemistry 21 (1982) 673–675.
[23] S. He, Y. Jang, P.F. Tu, Chemical constituents from *Cinnamomum cassia*, Zhongguo Zhong Yao Za Zhi 40 (2015) 3598–3602.
[24] Y. Du, N.F. Villeneuve, X.-J. Wang, Z. Sun, W. Chen, J. Li, H. Lou, P.K. Wong, D.D. Zhang, Oridonin confers protection against arsenic-induced toxicity through activation of the Nrf2-mediated defensive response, Environ. Health Perspect. 116 (2008) 1154–1161.
[25] A. Lau, S.A. Whitman, M.C. Jaramillo, D.D. Zhang, Arsenic-mediated activation of the Nrf2-Keap1 antioxidant pathway, J. Biochem. Mol. Toxicol. 27 (2013) 99–105.
[26] B.-J. Chen, C.-S. Fu, G.-H. Li, X.-N. Wang, H.-X. Lou, D.-M. Ren, T. Shen, Cinnamaldehyde analogues as potential therapeutic agents, Mini Rev. Med. Chem. 17 (2017) 33–43.
[27] F. Wang, P. Wang, J. Wan, J. Hou, P. Zhou, Cinnamaldehyde attenuates high glucose-induced oxidative stress and endothelial dysfunction as an Nrf2 activator, Atherosclerosis 252 (2016) e145.
[28] H. Zheng, S.A. Whitman, W. Wu, G.T. Wondrak, P.K. Wong, D. Fang, D.D. Zhang, Therapeutic potential of Nrf2 activators in streptozotocin-induced diabetic nephropathy, Diabetes 60 (2011) 3055–3066.
[29] Q. Ma, Role of Nrf2 in oxidative stress and toxicity, Annu. Rev. Pharmacol. Toxicol. 53 (2013) 401–426.
[30] D. Siegel, C. Yan, D. Ross, NAD(P)H: quinone oxidoreductase 1 (NQO1) in the sensitivity and resistance to antitumor quinones, Biochem. Pharmacol. 83 (2012) 1033–1040.
[31] S.L. Slocum, T.W. Kensler, Nrf2: control of sensitivity to carcinogens, Arch. Toxicol. 85 (2011) 273–284.
[32] H. Lv, Q. Liu, Z. Wen, H. Feng, X. Deng, X. Ci, Xanthohumol ameliorates lipopolysaccharide (LPS)-induced acute lung injury via induction of AMPK/GSK3β-Nrf2 signal axis, Redox Biol. 12 (2017) 311–324.
[33] S. Tao, Y. Zheng, A. Lau, M.C. Jaramillo, B.T. Chau, R.C. Lantz, P.K. Wong, G.T. Wondrak, D.D. Zhang, Tanshinone I activates the Nrf2-dependent antioxidant response and protects against As (III)-induced lung inflammation *in vitro* and *in vivo*, Antioxid. Redox Signal. 19 (2013) 1647–1661.
[34] A. Kode, S. Rajendrasozhan, S. Caito, S.-R. Yang, I.L. Megson, I. Rahman, Resveratrol induces glutathione synthesis by activation of Nrf2 and protects against cigarette smoke-mediated oxidative stress in human lung epithelial cells, Am. J. Physiol. Lung Cell Mol. Physiol. 294 (2008) L478–L488.
[35] A. Boutten, D. Goven, E. Artaud-Macari, J. Boczkowski, M. Bonay, NRF2 targeting: a promising therapeutic strategy in chronic obstructive pulmonary disease, Trends Mol. Med. 17 (2011) 363–371.
[36] H.-Y. Cho, S.R. Kleeberger, Nrf2 protects against airway disorders, Toxicol. Appl. Pharmacol. 244 (2010) 43–56.
[37] T. Müller, A. Hengstermann, Nrf2: friend and foe in preventing cigarette smoking-dependent lung disease, Chem. Res. Toxicol. 25 (2012) 1805–1824.
[38] A. Lau, S.A. Whitman, M.C. Jaramillo, D.D. Zhang, Arsenic-Mediated Activation of the Nrf2-Keap1 Antioxidant Pathway, J. Biochem. Mol. Toxicol. 27 (2013) 99–105.
[39] Z.-Y. Jiang, M.-C. Lu, L.L. Xu, T.-T. Yang, M.-Y. Xi, X.-L. Xu, X.-K. Guo, X.-J. Zhang, Q.-D. You, H.-P. Sun, Discovery of potent Keap1–Nrf2 protein–protein interaction inhibitor based on molecular binding determinants analysis, J. Med. Chem. 57 (2014) 2736–2745.
[40] R. Hancock, H.C. Bertrand, T. Tsujita, S. Naz, A. El-Bakry, J. Laoruchupong, J.D. Hayes, G. Wells, Peptide inhibitors of the Keap1–Nrf2 protein–protein interaction, Free Radic. Biol. Med. 52 (2012) 444–451.
[41] R. Hancock, M. Schaap, H. Pfister, G. Wells, Peptide inhibitors of the Keap1–Nrf2 protein–protein interaction with improved binding and cellular activity, Org. Biomol. Chem. 11 (2013) 3553–3557.
[42] H.-P. Sun, Z.-Y. Jiang, M.-Y. Zhang, M.-C. Lu, T.-T. Yang, Y. Pan, H.-Z. Huang, X.-J. Zhang, Q.-d. You, Novel protein–protein interaction inhibitor of Nrf2–Keap1 discovered by structure-based virtual screening, Med. Chem. Commun. 5 (2014) 93–98.
[43] L. Hu, S. Magesh, L. Chen, L. Wang, T.A. Lewis, Y. Chen, C. Khodier, D. Inoyama, L.J. Beamer, T.J. Emge, Discovery of a small-molecule inhibitor and cellular probe of Keap1–Nrf2 protein–protein interaction, Bioorg. Med. Chem. Lett. 23 (2013) 3039–3043.
[44] D. Sinha, J. Biswas, A. Bishayee, Nrf2-mediated redox signaling in arsenic carcinogenesis: a review, Arch. Toxicol. 87 (2013) 383–396.
[45] G. Marshall, C. Ferreccio, Y. Yuan, M.N. Bates, C. Steinmaus, S. Selvin, J. Liaw, A.H. Smith, Fifty-year study of lung and bladder cancer mortality in Chile related to arsenic in drinking water, J. Natl. Cancer Inst. 99 (2007) 920–928.
[46] J.E. Heck, A.S. Andrew, T. Onega, J.R. Rigas, B.P. Jackson, M.R. Karagas, E.J. Duell, Lung cancer in a US population with low to moderate arsenic exposure, Environ. Health Perspect. 117 (2009) 1718.
[47] T.R. Sanchez, M. Perzanowski, J.H. Graziano, Inorganic arsenic and respiratory health, from early life exposure to sex-specific effects: a systematic review, Environ. Res. 147 (2016) 537–555.
[48] C. Steinmaus, C. Ferreccio, J. Acevedo, Y. Yuan, J. Liaw, V. Durán, S. Cuevas, J. García, R. Meza, R. Valdés, Increased lung and bladder cancer incidence in adults after in utero and early-life arsenic exposure, Cancer Epidemiology and prevention, Biomarkers 23 (2014) 1529–1538.
[49] K. Jomova, Z. Jenisova, M. Feszterova, S. Baros, J. Liska, D. Hudecova, C. Rhodes, M. Valko, Arsenic: toxicity, oxidative stress and human disease, J. Appl. Toxicol. 31 (2011) 95–107.
[50] H. Wang, X. Li, T. Chen, W. Wang, Q. Liu, H. Li, J. Yi, J. Wang, Mechanisms of verapamil-enhanced chemosensitivity of gallbladder cancer cells to platinum drugs: glutathione reduction and MRP1 downregulation, Oncol. Rep. 29 (2013) 676–684.
[51] C. Cai, G. Qiu, X. Gong, Y. Chen, H. Zhao, Effects of erythromycin on γ-glutamyl cysteine synthetase and interleukin-1β in hyperoxia-exposed lung tissue of premature newborn rats, J. Pediatr. 90 (2014) 493–499.